

Quantum dot to quantum wire transition of m -plane GaN islands

B. Amstatt,^{1,2} J. Renard,¹ C. Bougerol,¹ E. Bellet-Amalric,¹ B. Gayral,¹ and B. Daudin¹

¹CEA-CNRS Group (Nanophysique et Semiconducteurs), SP2M, INAC, CEA Grenoble and Institut Néel/CNRS–Université J. Fourier, 17 rue des Martyrs, 38054 Grenoble, France

²NOVASiC, Savoie Technolac, Arche Bât. 4, BP 267, 73375 Le Bourget du Lac, France

(Received 6 June 2008; revised manuscript received 17 October 2008; published 13 January 2009)

Structural studies of m -plane GaN quantum dots and quantum wires are presented. A shape transition responsible for the evolution of quantum dots into quantum wires is put in evidence and shown to depend on the amount of material deposited. In addition, it is established that vertical correlation of successive nanostructure planes may also induce the dot-wire shape transition. Consistent with theoretical predictions, it is proposed that the shape transition results from an elastic energy minimization process made possible by an easy adatom diffusion along $[11-20]$ direction.

DOI: 10.1103/PhysRevB.79.035313

PACS number(s): 68.55.ag, 81.15.Hi

I. INTRODUCTION

The instability of strained layers has been recognized for many years and has been the basis of numerous experimental and theoretical works in the past decades. In such a context, special attention has been paid to strain relaxation mechanisms, which are based on dislocation formation or shape instability. The case of shape instability is of particular interest, resulting in the formation of low dimension quantum dots (QDs) or quantum wires (QWires). More precisely, the so-called Stranski-Krastanow (SK) growth mode has been identified as a mechanism in which a strained two-dimensional layer abruptly converts into three-dimensional (3D) islands above a given critical thickness in order to relax its elastic energy thanks to free-surface formation. Moreover, it was theoretically predicted by Tersoff and Tromp¹ that a shape transition from roughly symmetric islands to markedly elongated ones may be observed, depending on island size and provided the surface adatom diffusion is sufficient. These predictions have satisfactorily accounted for the experimental results observed in the case of CoS₂ clusters on Si (100) (Ref. 2) or of Pb on Si (111),³ to limit ourselves to a few significant examples.

Now restricting ourselves to the case of nitride semiconductors, the SK growth mode of (0001) (c plane) GaN on c -plane AlN has been put in evidence using both molecular-beam epitaxy (MBE) (Refs. 4 and 5) and metal organic chemical vapor deposition (MOCVD) (Ref. 6) techniques. Interestingly, GaN/AlN system is free of interdiffusion, making it particularly relevant to study strain relaxation mechanisms.⁷ In particular, it has been found that surface energy may play a major role and that in growth conditions associated with the formation of a continuous Ga layer on growing GaN, the 3D island formation is totally inhibited.⁸ In such a case, strain relaxation occurs through dislocation formation, according to the well-known Frank–Van der Merwe growth mode.⁹ This is direct evidence that surface energy may change the energetical hierarchy between dislocation and island formation. Then as a practical consequence of major importance for applications, either GaN quantum dots or quantum wells (QWs) can be grown on AlN or Al-GaN by properly controlling experimental conditions.¹⁰

In addition to these results $[11-20]$ (a plane) and $[1-100]$ (m plane) GaN QDs have been recently grown.^{11,12} Again, it has been found that depending on growth conditions either nonpolar GaN QDs or QWs may be grown. The practical interest in these nonpolar heterostructures is due to the expected reduction or suppression of the internal electric field, which results from a combination of both spontaneous and piezoelectric polarizations¹³ and may lead to a reduced radiative recombination efficiency in c -plane oriented heterostructures, detrimental to applications.¹⁴

In the case of m -plane GaN nanostructures, it has been further found that either QDs or QWires can be obtained depending on the strain state of the m -plane AlN buffer layer deposited on m -plane SiC before GaN growth.¹² The main result of this work was to establish that the shape of m -plane GaN nanostructures grown on m -plane AlN was imposed by the strain asymmetry of the AlN surface more than by equilibrium conditions proper to GaN island itself. By contrast, it was alternately observed that in the case corresponding to QDs formation, increasing the amount of GaN deposited eventually led to a shape transition from QDs to QWires. In this case, it is expected that the change in shape from QD to QWire is not related to the asymmetry of the AlN but rather results from a competition between surface energy and strain energy, making the island adopt an almost isotropic shape below a critical amount of material deposited and an anisotropic shape above this critical amount. It is the aim of the present paper to study this transition in detail. It will be established that it depends on the amount of GaN deposited but can alternately be induced by vertical correlation of nanostructures in stacked planes, depending on the thickness of the spacer between successive planes. Eventually, it will be demonstrated that the transition from QDs to QWires is consistent with the model proposed by Zandvliet and van Gestel,¹⁵ as an illustration of a strain relaxation mechanism made possible in the present case by anisotropic strain state of GaN islands combined with an easy surface diffusion along $[11-20]$, large enough to favor island elongation.

II. SAMPLES

The samples were grown by plasma-assisted MBE on commercial (1-100) SiC substrates polished at the monolayer

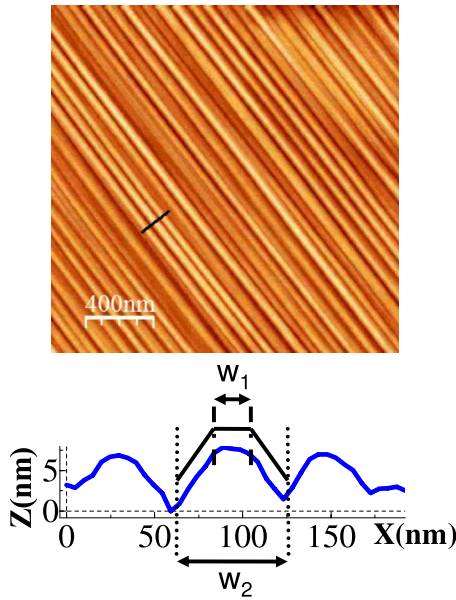


FIG. 1. (Color online) (a) AFM image of a 300-nm-thick AlN buffer layer on *m*-plane SiC. (b) Profile of the undulations along *x* axis.

scale by NOVAsiC Company,¹⁶ i.e., the active N source was produced by dissociation of N_2 in a rf-plasma cell. After chemical cleaning, the substrate was fixed with In on a molybdenum sample holder and introduced in the growth chamber. Then an AlN buffer layer was deposited, before growth of GaN. The AlN buffer thickness was about 300 nm, large enough to ensure formation of GaN QDs, according to the Stranski-Krastanow growth mode.¹²

A first series of samples was grown to study the morphological transition of GaN nanoislands as a function of GaN content. The samples of this series each consisted of one plane of GaN of variable thickness, namely, 5, 7, 15, and 20 monolayers (ML), which was deposited on the AlN buffer. Next this layer was capped with about 20 nm of AlN and a second plane of GaN of same thickness as the first one was deposited and let uncovered for atomic force microscopy (AFM) experiments.

A second series was grown to specifically study the effect of vertical correlation on GaN nanostructure morphology. Each sample of this series consisted of a superlattice of 25 GaN/AlN bilayers deposited on a 300 nm AlN buffer layer. Each GaN plane corresponded to 5 ML of material deposited. The AlN spacer between successive GaN planes was 3, 15, and 22 nm thick (note that 1 ML \approx 0.25 nm). The last GaN plane was left uncovered to make possible AFM experiments and study the GaN island morphology as a function of AlN spacer thickness.

A third series of samples was grown to study how vertical correlation progressively leads to the formation of GaN QWires when starting from QDs. Samples of this series consisted of a stacking of GaN/AlN bilayers. Each GaN plane corresponded to 5 ML of material deposited and the AlN spacer thickness was chosen small enough to lead to vertical correlation, i.e., 3 nm. In this series, the number of GaN/AlN bilayers was 2, 3, or 5. The last GaN plane was left uncov-

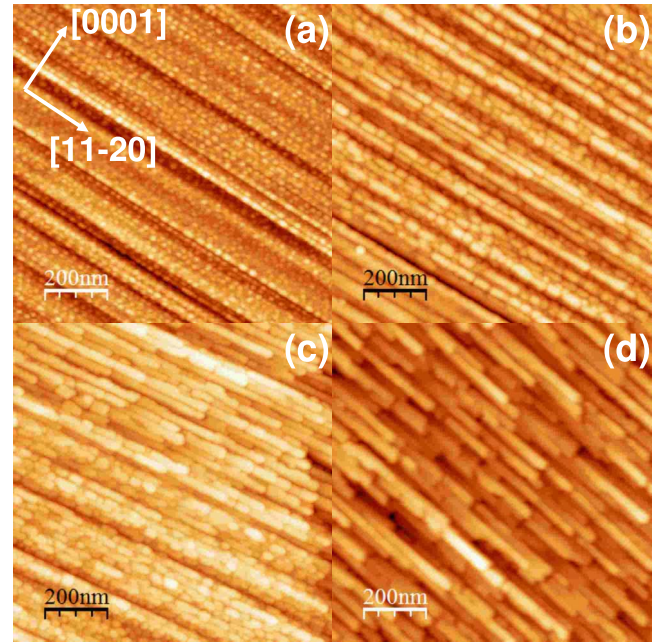


FIG. 2. (Color online) $1 \times 1 \mu\text{m}^2$ AFM images showing GaN islands deposited on a 300-nm-thick AlN buffer layer, as a function of GaN amount. (a) 5, (b) 7, (c) 15, and (d) 20 ML.

ered to make possible AFM experiments in order to determine the number of bilayers necessary to reach the steady regime corresponding to vertical correlation.

All AFM measurements presented in this paper were performed on the surface plane in a Dimension 3100 AFM operated in tapping mode. An AFM picture of an AlN buffer layer of thickness equal to that used in the present study is shown in Fig. 1(a). It exhibits stripes elongated along [11-20]. This morphology and the associated undulations put in evidence in Fig. 1(b) are assigned to the partial strain relaxation of AlN anisotropically strained on *m*-plane SiC.¹² Two characteristic dimensions are defined in Fig. 1(b), namely, the nearly flat top of the undulations, W_1 , typically 25 ± 5 nm wide, and the width of AlN stripes, W_2 , equal to about 75 ± 10 nm.

III. RESULTS

Dot to wire transition as a function of GaN amount

The evolution of *m*-plane GaN nanostructures as a function of GaN amount deposited, which ranged from 5 to 20 ML, has been studied by AFM (Fig. 2). Starting from QDs, a transition towards wire morphology is observed for a GaN amount larger than 5 ML. Coexistence between dots and wires is observed for a GaN amount up to 15 ML. Above 15 ML, only wires are observed.

At this stage, it is worth recalling that GaN QDs exhibit various morphologies, depending on crystallographic orientation: *c*-plane GaN QDs are hexagonal truncated pyramids,⁴ whereas *a*-plane GaN QDs exhibit a trapezoidal shape.¹¹ In contrast, *m*-plane GaN QDs here studied have a rectangular shape, with the long side along [11-20]. This leads to the definition of an in-plane aspect ratio, L/w , where L is the

nanoisland dimension along $[11-20]$ and w is the dimension along $[0001]$. This aspect ratio typically varies between 1.5 and 2 for m -plane QDs. For increasing amount of material deposited, the transition from QDs to QWires is characterized by a *discrete jump* in the aspect ratio value which abruptly shifts from 2 to 3. We then defined m -plane QDs as nanoislands with an in-plane aspect ratio strictly inferior to 2 and m -plane QWires as objects with an in-plane aspect ratio larger than 2. In the growth conditions explored in the present study, the QWires in-plane aspect ratio was between 3 and 5.

Let us note that the QDs/QWires denomination that we use in this paper refers to *morphological* properties. Actually, as far as electronic properties are concerned, both QDs and QWires have large widths and lengths compared to the GaN Bohr radius (2.8 nm), so that quantum confinement properties are mostly governed by the height of the nanostructures whereas the in-plane confinement will be weak in both cases along both axes. Indeed, we have recently shown that at low temperature, the photoluminescence properties of m -plane QDs and QWires are very similar.¹⁷

As mentioned above, it has to be emphasized that the phenomenology illustrated in Fig. 2 is different from results previously reported where the formation of either QDs or QWires was correlated with the strain state of subjacent AlN buffer layer. In such a case, QWires formation was found to occur *independently* of the amount of GaN deposited, which has been assigned to strain anisotropy of AlN buffer layer grown on (1-100) SiC.¹² By contrast, it is worth stressing again that in all experiments reported in the present paper the AlN buffer layer was thick enough to be partially relaxed, a situation corresponding to the formation of QDs in the first stages of nanostructure nucleation,¹² followed by wire formation as shown in Fig. 2 for increasing amount of GaN deposited. Then, in this case, it is expected that the change in shape from QD to QWire is not related to the asymmetry of the AlN buffer layer but rather results from a competition between surface energy and strain energy, as it will be later discussed.

High-resolution transmission electron microscopy images (HRTEM) of the studied nanoislands were obtained on a Jeol 4000EX microscope operated at 400 kV. Samples were prepared in cross sections by mechanical polishing followed by ion milling and observed along $[11-20]$ and $[0001]$ zone axes. Figure 3(a) is a HRTEM image of an m -plane GaN QWire viewed along the $[11-20]$ zone axis. It has been previously shown that no apparent difference exists between QDs and QWires when viewed along this zone axis, which is characterized by a profile asymmetry assigned to the polar nature of c axis.¹² More precisely, it has been demonstrated that the $+c$ axis (corresponding to the Ga-face polarity of (0001) material) points towards the less abrupt facet, whereas the $-c$ axis (corresponding to the N-face polarity of (0001) material) points towards the most abrupt facet.¹⁸

Features in Fig. 3(a), namely, the absence of well-defined facets on the $+c$ side of nonpolar GaN QDs/QWires, suggest that, following nucleation, nanostructure growth preferentially occurs in $+c$ direction when increasing the amount of GaN deposited. Such a hypothesis is consistent with previous results on GaN grown by MOCVD showing that Ga-polar

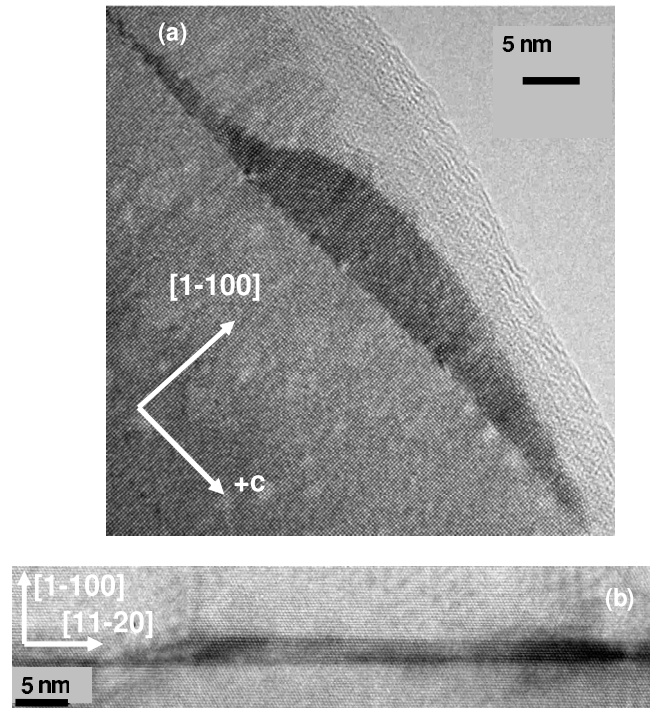


FIG. 3. High-resolution transmission microscopy images of m -plane GaN quantum wires corresponding to 15 ML of GaN deposited. (a) HREM of a GaN QWire taken along the $[11-20]$ zone axis, showing the anisotropic wire shape correlated with the direction of c polar axis. The sharp edge corresponds to $+c$. (b) HREM taken along the $[0001]$ zone axis, showing the needle shape morphology of a GaN quantum wire.

inversion domains (with $+c$ direction, i.e., a Ga-polar growth front) grow faster than the surrounding N-polar matrix.¹⁹ This conclusion is also supported by results on the growth of free-standing GaN platelike crystals in thermodynamic equilibrium conditions. In such a case, it has been found that growth mostly occurs on Ga-terminated face while growth of N-terminated face is almost negligible.²⁰ Moreover, and more comparable to MBE out of thermodynamical equilibrium conditions, a study of epitaxial lateral overgrowth (ELOG) of (1-100) m -plane GaN in MOCVD has established that growth on Ga-terminated facets is faster than growth on N-terminated facets.²¹

In the case of $[1-100]$ GaN QDs, although no Ga-terminated or N-terminated facets are observed, it should be noted that atomic steps are differently terminated depending on the c -axis direction. The above results suggest that in the Ga-rich growth conditions used for growing $[1-100]$ GaN QDs,¹² their morphology is dominated by the easy incorporation of impinging adatoms on the $+c$ related growth front, whereas incorporation on the $-c$ related growth front is less probable.

Figure 3(b) shows a GaN QWire, viewed along the $[0001]$ zone axis. It exhibits a needle-shaped morphology, suggesting an easy diffusion along $[11-20]$. Note that height is varying along the length of the wire. Because of nonpolar character of $\langle 11-20 \rangle$ direction, it is not expected that the growth rate is different along $[11-20]$ and $[-1-120]$. Accordingly, this anisotropic shape of wires cannot be assigned to wurtzite

crystallographic symmetry but has been rather assigned to vicinality component of (1-100) SiC substrate along [11-20] direction.²²

Statistical analysis of AFM images has been performed allowing one to determine the length L (dimension along [11-20] direction), the width w (dimension along [0001] direction), and the height h of GaN nanostructures as a function of GaN coverage. For that purpose, about 100 nanoislands were analyzed for each studied sample, corresponding to a nominal amount of deposited GaN varying between 3 and 40 ML. For each nanoisland L and w were measured. Error bars in Fig. 4 (and later in Figs. 5 and 8) correspond to the full width at half maximum of the Gaussian used to fit the distribution of the data over the 100 objects studied.

Results are reported in Fig. 4. They reveal [Figs. 4(a) and 4(b)] a marked transition between dot and wire regimes as far as length and width are concerned. Both are found to increase proportionally to GaN coverage θ , obeying the expressions

$$L_i = a_i \theta + b_i, \quad (1)$$

$$w_i = a'_i \theta + b'_i, \quad (2)$$

where i refers to QDs or QWires. According to a linear mean-square fit of the data, it is found that $a_{\text{QD}}=2.5$ nm/ML, $a_{\text{QWires}}=6$ nm/ML, with $b_{\text{QD}}=15$ nm and $b_{\text{QWires}}=37$ nm. Similarly, it is found that $a'_{\text{QD}}=a'_{\text{QWires}} \sim 2$ nm/ML, with $b'_{\text{QD}}=15$ nm and $b'_{\text{QWires}}=0.5$ nm. From these data, it is concluded that dot size increases almost isotropically as a function of θ . Interestingly, the maximum dot width appears to be related to the morphology of AlN buffer layer. More precisely, the maximum dot width corresponds to W_1 [see Figs. 1 and 4(b)], the top of AlN stripes. By contrast, in the wire growth regime, it is found that a_{QWires} is about three times larger than a'_{QWires} , as a clear indication of an easy growth along [11-20] in this regime. It is worth noting that the QWire width tends to W_2 , the width of AlN buffer stripes. Further increase in the amount of GaN deposited leads to the formation of a continuous, rough GaN layer. In Fig. 4(c), it is shown that h slowly increases as a function of GaN coverage, with no singularity observable between dot and wire growth regimes. A saturation is observed for $h=2.5$ nm.

As clearly shown in Fig. 4(a), a gap is observed in the variation in the length of the nanostructures as a function of the amount of GaN deposited, as a clue that the dot-wire transition is abrupt and does not correspond to a continuous and isotropic evolution of dot size. Then, as a more precise definition of what QDs and QWires are, it appears from quantitative results reported in Fig. 4 that QDs exhibit an almost isotropic increase in size. Their L/w in-plane aspect ratio is smaller than 2, this moderate elongation along [11-20] being tentatively assigned to the strain asymmetry. The transition toward QWires shows a marked departure from this regime: following the abrupt increase in length associated to the transition, w is almost constant while L rapidly increases as a function of deposited GaN amount. QWire regime is characterized by this fully anisotropic

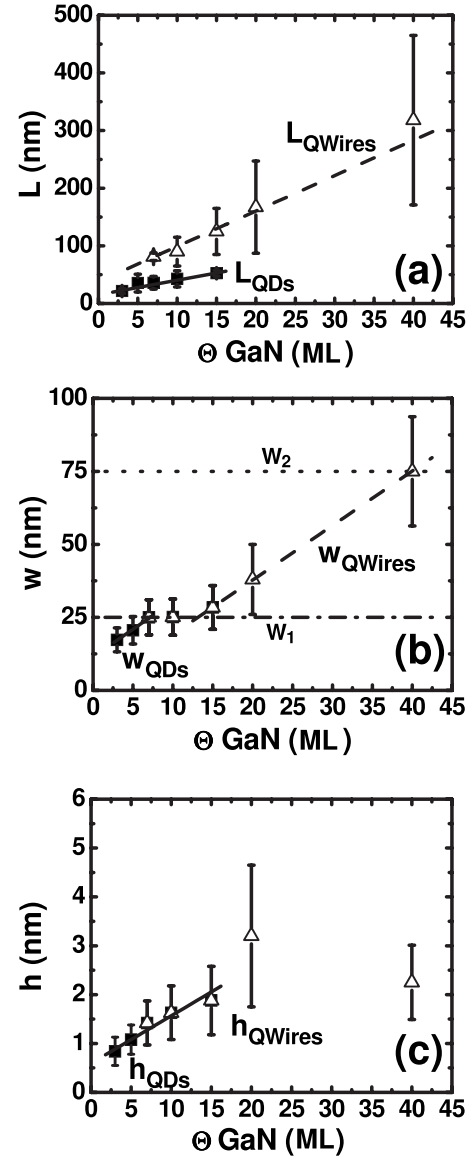


FIG. 4. Statistics of (a) length (L), (b) width (w), and (c) height (h) of m -plane GaN quantum dots and quantum wires extracted from AFM images shown in Fig. 2. Solid squares: QDs; open triangles: QWires. Note that height does not depend on island morphology and saturates to a value of about 2.5 nm. In (b), the dash-dotted line corresponds to W_1 , the top width of AlN stripes shown in Fig. 1, and the dotted line corresponds to W_2 , the mean width of AlN stripes.

growth up to about 15 ML of deposited GaN, which is made possible by kinetics, leading nanostructures to adopt a strongly anisotropic shape.

Quantitative results extracted from statistical analysis, namely, L and w , have been reported in Fig. 5 as a function of the area covered by the nanostructures, i.e., the quantity $A=Lw$. Below $A=1500$ nm², corresponding to QDs only, a unique regime is found. By contrast, above $A=1500$ nm², an abrupt change is observed, assigned to a shape transition from dots to wires, i.e., to a marked shape anisotropy transition.

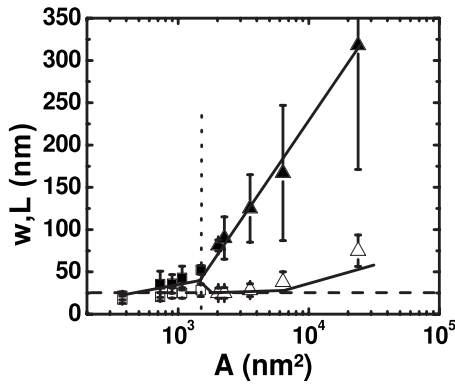


FIG. 5. Width w (open squares and open triangles for QDs and QWires, respectively) and length L (solid squares and solid triangles for QDs and QWires, respectively) of GaN islands as a function of their area, from data in Fig. 4. The vertical dotted line at $A=1500 \text{ nm}^2$ corresponds to the critical area for the transition from dots to wires.

IV. EFFECT OF VERTICAL CORRELATION

In a next set of experiments, the effect of vertical correlation of m -plane nanostructures on their morphology was studied. As it will be shown below, it was found that vertical correlation induces a transition from QDs to QWires. It is the aim of this section to present and comment on these features.

Samples have been described in Sec. II. It has to be recalled that the AlN buffer thickness, 300 nm, was chosen to ensure formation of QDs when depositing GaN on it.¹² Figures 6(a)–6(c) show AFM pictures of the on-surface plane as a function of the spacer thickness between each of the 25 GaN dot planes (5 ML GaN nominally deposited), namely, 3, 15, and 22 nm, respectively. In the case of Fig. 6(c) corresponding to a spacer of 22 nm, only dots are observed in the surface, consistent with the experimental evidence that partially relaxed AlN buffer leads to formation of GaN QDs and furthermore suggesting that the morphology of the surface plane is not influenced by the presence of those previously deposited. In contrast, a thinner buffer yields to the observation in the surface of a coexistence of dots and wires (15 nm AlN spacer) or of wires only (3 nm AlN spacer), strongly suggesting that the morphology change with respect to the case of a 22-nm-thick AlN buffer results from the influence of previously deposited GaN planes, which is tentatively assigned to a vertical correlation effect.

Next, with the aim of clarifying the mechanism leading to a transition from dot to wire morphology in the case of superlattices, the AlN buffer layer thickness was fixed to 3 nm, which eventually gives rise to formation of wires after stacking 25 GaN planes as shown above. Now the number of stacked planes was varied between 1 and 25. Figure 7(a)–7(c) show the result for 2, 3, and 5 planes, respectively. It appears that coexistence between dots and wires is already observed for a stack of 3 planes, the fraction of wires regularly increasing for a greater number of stacked planes. The statistical analysis results in Fig. 8(a) show that the density of nanostructures (dots and/or wires) is rapidly decreasing as a function of the number of stacked planes while their area is

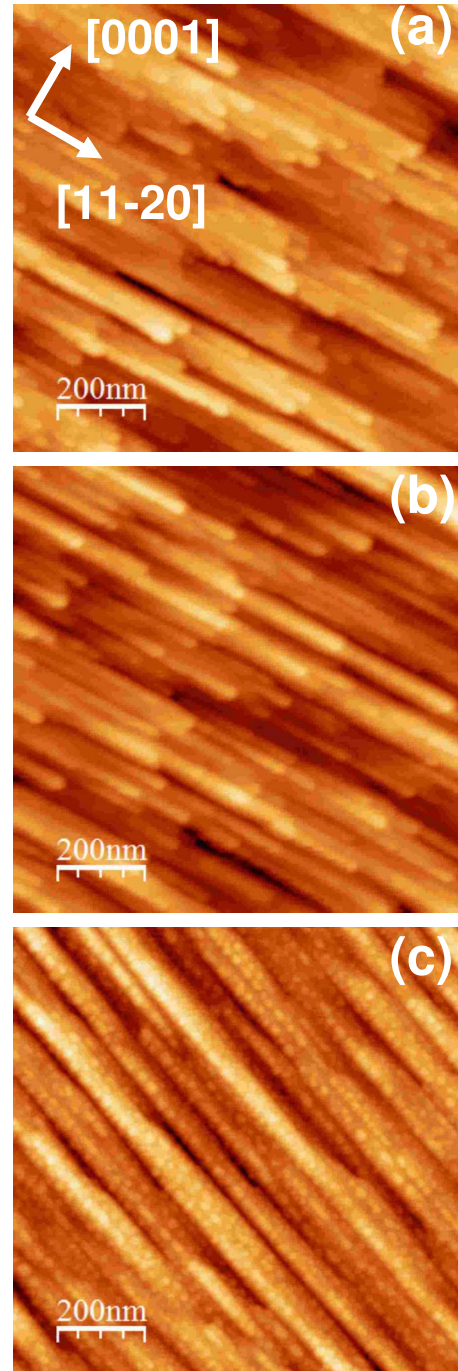


FIG. 6. (Color online) $1 \times 1 \mu\text{m}^2$ AFM images of the surface plane of a superlattice consisting of 25 planes of GaN islands separated by an AlN spacer (a) 3, (b) 15, and (c) 22 nm thick. The amount of GaN deposited corresponds to 5 ML.

increasing and then saturating between 4 and 25 planes. Such a phenomenology, namely, a size filtering correlated with a density decrease, is typical of vertical correlation, as theoretically analyzed by Tersoff *et al.*²³ in the case of QDs. These considerations are further supported by TEM observations along the [0001] zone axis (not shown here) which have put in evidence vertical correlation of wires for an AlN spacer of 4 nm between successive planes. As the quantity of GaN nominally deposited, namely, 5 ML, is constant, it is

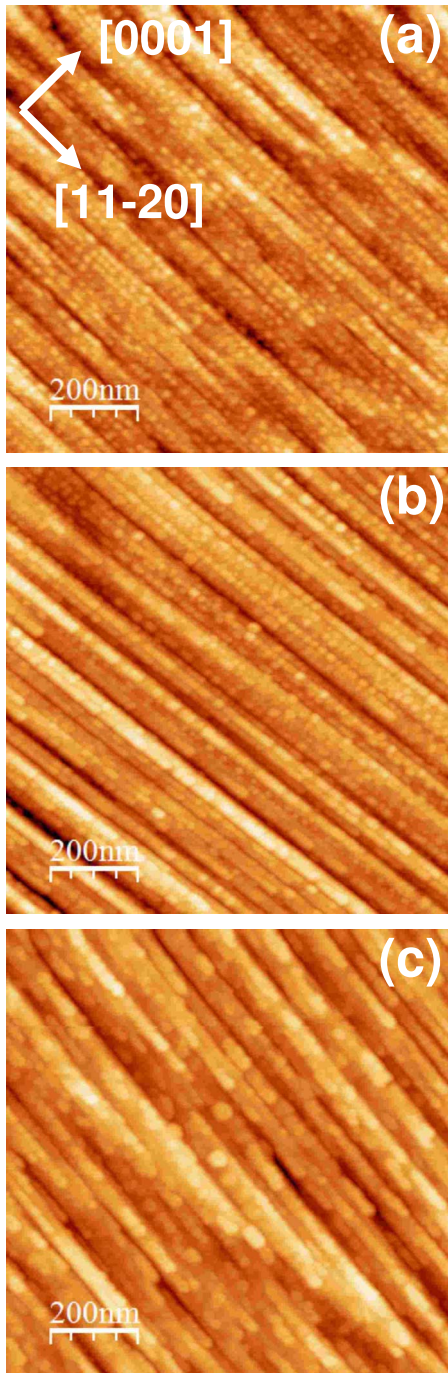


FIG. 7. (Color online) $1 \times 1 \mu\text{m}^2$ AFM images of the surface plane of a superlattice of correlated GaN islands (AlN spacer thickness equal to 3 nm) as a function of the number of planes of the superlattice, N : (a) $N=2$, (b) $N=3$, and (c) $N=5$.

reasonable to assume that also in the present case the decrease in nanostructures density as well as their size increase as a function of the number of stacked planes leads to a redistribution of GaN material, eventually resulting locally in an amount sufficient to trigger the dot-wire transition.

This statement is supported by results reported in Fig. 8(b) which were obtained by plotting L and w as a function of area for the various nanostructures corresponding to Figs. 7(a)–7(c). Again, a dot-wire transition as a function of area is

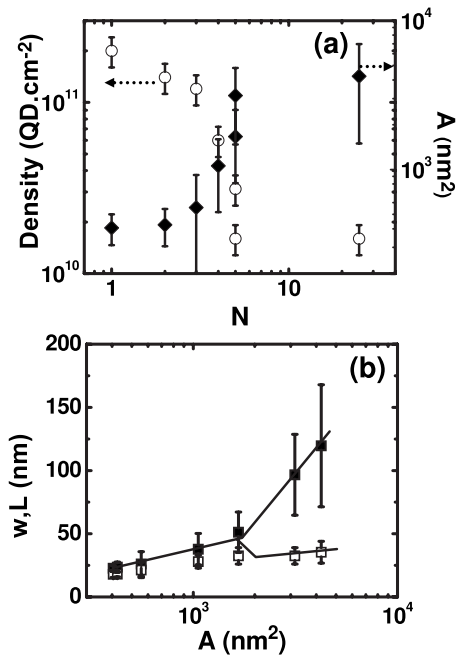


FIG. 8. (a) Evolution of the density (open circles) and area A (solid diamonds) of the GaN nanostructures with the number of correlated planes, N . (b) Evolution of w (open squares) and L (solid squares) of GaN nanostructures as a function of their area.

put into evidence, consistent with the arguments of Tersoff and Tromp.¹ Interestingly, experimental data in Fig. 8(b) can be superimposed to those in Fig. 5. In particular, the critical area for dot-wire transition is also found to be about 1500 nm^2 . We then conclude that the dot-wire transition in the case of correlated superlattices simply results from GaN material accumulation on selected nucleation sites, locally leading to a quantity deposited large enough to result in wire formation, as observed in Fig. 2.

V. DISCUSSION

Experiments reported above put into evidence a shape transition of [1-100] GaN QDs into QWires as a function of the amount of GaN deposited. In first approximation, these results are consistent with the model of Tersoff and Tromp¹ predicting that stored elastic energy is best relaxed through such a shape transition. It should be emphasized that this model assumes that dot to wire transition is a smooth one, i.e., with a continuous change from one shape to another. Such a model accounts satisfactorily for the results reported by Brongersma *et al.*² concerning the spontaneous transition from square shape clusters of CoS_2 deposited on Si(100) into elongated ones. However, the case of (1-100) GaN nanoislands described above differs from the one of CoS_2 by the fact that bimodality is observed, namely, a coexistence of dots and wires between 7 and 15 ML of GaN coverage, associated with a gap in the evolution of nanostructure length as a function of the amount of GaN deposited.

Recently, the possibility of a sharp transition, with an abrupt change from a dot shape to a wire one, was theoretically analyzed by Zandvliet and van Gastel.¹⁵ These authors

considered the case of islands with monopole forces acting on neighboring boundaries pointing in opposing directions and established that it led to a coexistence of compact and elongated islands.

It should be noted that (1-100) GaN surface contains an equal number of threefold coordinated N and Ga atoms, which makes charge neutrality possible without reconstruction.²⁴ Nevertheless, it is possible that an anisotropic surface stress associated with deformation along c direction of surface Ga-N dimer be the driving force triggering dot to wire transition according to the model proposed by Zandvliet and van Gastel.¹⁵ Moreover, it should be noted that the deposited GaN material is far from elastic equilibrium as a consequence of its heteroepitaxy on AlN and that it consequently experiences a strongly anisotropic elastic strain.

We conclude from the results in Fig. 2 and 3 that the morphology of [1-100] GaN nanostructures results from the combined action of three very different growth rates along $+c$, $-c$, and [11-20]: following nucleation, growth preferentially occurs along $+c$ while it is negligible along $-c$. Consistent with results in Fig. 4, it is suggested that dot nucleation likely occurs on top of AlN stripes, in the region labeled W_1 in Fig. 1. This region corresponds to a locally enhanced elastic strain relaxation of AlN, making nucleation of GaN more favorable. Such a hypothesis is consistent with a saturation of dot width to 25 nm, which corresponds to W_1 . Next, further deposition of GaN results in a preferential growth along [11-20]. This phenomenological scenario is supported by experimental evidence extracted from ELOG data obtained using masks with star-patterned openings.²⁵ A trend for maximum lateral growth for stripes extending along [1-100] direction has been observed, as an indication of a favored growth along [11-20] direction (perpendicular to stripe opening direction) and of a maximum value of [11-20] direction/[0001] direction growth rate ratio. Then, in the stage corresponding to growth along [11-20], which is not only favored by easy diffusion but also not limited by the presence of adjacent rows, the progressive size increase in the islands is followed by a shape transition, according to the theoretical predictions.^{1,15}

The above considerations are consistent with recent calculations of the Ga adatom surface diffusion barriers on a -plane and m -plane GaN. These calculations have put in evidence the anisotropic character of Ga diffusion on m -plane surface associated to a surface diffusion barrier more than four times smaller along [11-20] than along [0001].²⁶ As a consequence, it is expected that Ga diffusion along [11-20] should be easy, consistent with the possibility to form wires elongated along this peculiar direction.

Interestingly, a -plane GaN QDs also exhibit in-plane alignment, perpendicular to c axis. The morphology of these a -plane GaN QDs was found to be asymmetric, which was correlated with the orientation of c axis.¹¹ However, increasing the amount of GaN deposited did not lead in this case to a shape transition, contrary to the case of m -plane QDs examined here. Although the presence of adjacent rows of dots also limited the extension of a -plane GaN QDs along c direction while potentially favoring a size increase along [1-100], no shape transition was observed but eventually, a coalescence of the dots. It has been theoretically calculated

that surface energies of a -plane and m -plane GaN are similar, namely, 123 and 118 meV/Å², respectively.²⁴ Then it is unlikely that surface energy is responsible for the absence of dot-wire transition in the case of a -plane GaN QDs, rather suggesting that easy diffusion along [11-20] is indeed a decisive condition to account for the shape transition observed in the case of m -plane QDs. As pointed out by Tersoff and Tromp,¹ diffusion must be sufficient to let the growing island reach the critical size for dot-wire transition. Insufficient diffusion along [1-100] is consistent with the formation of a -plane QDs and their coalescence for increasing amount of GaN deposited.²⁷ Again, this speculation is well supported by the results in Ref. 26, which has established that [1-100] is not an easy diffusion direction for Ga on a plane. By contrast, easy diffusion along [11-20] on the m -plane surface leads to the rapid size increase of dots, till reaching the critical size of 1500 nm², onset for dot-wire transition.

It should be remarked at this stage that the discrepancies between the simplified dot shape assumed in theoretical models and the real shape of m -plane GaN islands make difficult a quantitative analysis of the experimental results. As a matter of fact, m -plane GaN QDs and QWires viewed along [11-20] zone axis in high-resolution electron microscopy exhibit a marked asymmetric shape related to the polar character of c axis.²⁸ Moreover and also related to the polar character of c axis, it is expected that the chemical termination of facets oriented along $+c$ or $-c$ will differ and lead to different surface energies. More generally, the lack of data on high index surface energies in nitrides still is a serious limitation to quantitative analysis of results. It should also be noted that AlN anisotropic morphology is likely responsible for the limited growth rate along $+c$, as suggested by experimental results in Figs. 1 and 4. As a consequence, GaN islands tend to adopt a nonsymmetric shape before occurrence of dot-wire transition, with their length L along [11-20] larger than their width w along [0001]. More precisely, data in Figs. 4(a) and 4(b) show that L evolves faster than width, with an increased asymmetry between 7.5 and 15 ML of deposited GaN. In this GaN coverage range, the island aspect ratio, defined by Zandvliet *et al.*¹⁵ as $c^2=L/w$, progressively evolves from 1.15 to about 2. It is then suggested that this aspect ratio increase, which leads to an increased instability of dotlike islands, could be one triggering parameter for dot-wire transition, in addition to the size increase above the critical value.

As an alternative mechanism accounting for dot to wire transition, it has been theoretically established that strain anisotropy could remove the shape instability of a strained island, predicting a preferential growth along the less strained direction.²⁹ Indeed, m -plane GaN exhibits an anisotropic mismatch with respect to relaxed m -plane AlN, namely, 2.45% along [11-20] and 4.08% along [0001]. At first sight, such an anisotropic mismatch should favor growth along [11-20], which is effectively observed. However, it has been recently established that the effective mismatch of GaN islands grown on AlN differs from theoretical value due to the strain state of AlN on m -plane SiC and to an anisotropic elastic strain relaxation of GaN, which was found to be easier along [0001], a feature which is partly mediated by the large density of stacking faults eventually associated to partial dislo-

cations at the AlN/GaN interface.³⁰ The formation of these partial dislocations is associated to growth along $+c$ direction and it contributes to reverse the strain state anisotropy of GaN on AlN. We then speculate that during the step corresponding to growth along $[11-20]$ GaN actually experiences a larger strain along $[11-20]$ than along $[0001]$. This further supports the tentative conclusion that the wire formation along $[11-20]$ is of kinetical rather than from thermodynamic origin, consistent with the fact that usual growth temperature of GaN by MBE is out of thermodynamical equilibrium conditions.

In summary, we have shown that m -plane GaN nanostructures exhibit a shape transition from compact to elongated when increasing the amount of GaN deposited. Whereas a complete quantitative description is made difficult by both

the complex morphology of m -plane GaN islands and the lack of quantitative data on high index surface energies, it is remarkable that the phenomenology of this transition is qualitatively in agreement with theoretical predictions. In particular, the existence of a coexistence regime between dots and wires has been established, which has been tentatively assigned to the specific nucleation process in the present case. The experimental evidence that elastic relaxation of strained m -plane GaN semiconductor nanostructures may be efficiently assisted by a shape transition has added a new member to the family of materials exhibiting this behavior, which tends to indicate that the mechanism is quite general, provided that surface diffusion is large enough to make it possible.

-
- ¹J. Tersoff and R. M. Tromp, Phys. Rev. Lett. **70**, 2782 (1993).
²S. H. Brongersma, M. R. Castell, D. D. Perovic, and M. Zinke-Allmann, Phys. Rev. Lett. **80**, 3795 (1998).
³R. van Gastel, N. C. Bartelt, and G. L. Kellogg, Phys. Rev. Lett. **96**, 036106 (2006).
⁴B. Daudin, F. Widmann, G. Feuillet, Y. Samson, M. Arlery, and J. L. Rouvière, Phys. Rev. B **56**, R7069 (1997).
⁵B. Damilano, N. Grandjean, F. Semond, J. Massies, and M. Leroux, Phys. Status Solidi B **216**, 451 (1999).
⁶M. Miyamura, K. Tachibana, T. Someya, and Y. Arakawa, J. Cryst. Growth **237-239**, 1316 (2002).
⁷E. Sarigiannidou, E. Monroy, B. Daudin, and J. L. Rouvière, Appl. Phys. Lett. **87**, 203112 (2005).
⁸N. Gogneau, D. Jalabert, E. Monroy, T. Shibata, M. Tanaka, and B. Daudin, J. Appl. Phys. **94**, 2254 (2003).
⁹J. H. Van der Merwe, J. Appl. Phys. **34**, 123 (1963).
¹⁰B. Gayral and B. Daudin, in *Handbook of Self Assembled Semiconductor Nanostructures*, edited by M. Henini (Elsevier, New York, 2008).
¹¹S. Founta, C. Bougerol, P. Vennéguès, H. Mariette, and B. Daudin, J. Appl. Phys. **102**, 074304 (2007).
¹²B. Amstatt, J. Renard, C. Bougerol, E. Bellet-Amalric, B. Gayral, and B. Daudin, J. Appl. Phys. **102**, 074913 (2007).
¹³F. Bernardini and V. Fiorentini, Phys. Rev. B **57**, R9427 (1998).
¹⁴A. D. Andreev and E. P. O'Reilly, Appl. Phys. Lett. **79**, 521 (2001).
¹⁵H. J. W. Zandvliet and R. van Gastel, Phys. Rev. Lett. **99**, 136103 (2007).
¹⁶NOVASiC, Savoie Technolac-Arche Bât. 4, BP 267, 73375 Le Bourget du Lac Cedex, France (sales@novasic.com).
¹⁷J. Renard, B. Amstatt, C. Bougerol, E. Bellet-Amalric, B. Daudin, and B. Gayral, J. Appl. Phys. **104**, 103528 (2008).
¹⁸J. L. Rouvière, C. Bougerol, B. Amstatt, E. Bellet-Amalric, and B. Daudin, Appl. Phys. Lett. **92**, 201904 (2008).
¹⁹J. L. Rouvière, M. Arlery, R. Niebuhr, K. H. Bachem, and O. Briot, MRS Internet J. Nitride Semicond. Res. **1**, 33 (1996).
²⁰E. Frayssinet, W. Knap, S. Krukowski, P. Perlin, P. Wisniewski, T. Suski, I. Grzegory, and S. Porowski, J. Cryst. Growth **230**, 442 (2001).
²¹B. A. Haskell, T. J. Baker, M. B. McLaurin, F. Wu, P. T. Fini, S. P. DenBaars, J. S. Speck, and Shuji Nakamura, Appl. Phys. Lett. **86**, 111917 (2005).
²²B. Amstatt, Ph.D. thesis, Université Joseph Fourier, Grenoble (France), 2008.
²³J. Tersoff, C. Teichert, and M. G. Lagally, Phys. Rev. Lett. **76**, 1675 (1996).
²⁴J. E. Northrup and J. Neugebauer, Phys. Rev. B **53**, R10477 (1996).
²⁵G. Nataf, B. Beaumont, A. Bouillé, S. Haffouz, M. Vaille, and P. Gibart, J. Cryst. Growth **192**, 73 (1998).
²⁶L. Lymperakis and J. Neugebauer (unpublished).
²⁷S. Founta, Ph.D. thesis, Université Joseph Fourier, Grenoble (France) 2007.
²⁸J.-L. Rouvière, C. Bougerol, B. Amstatt, E. Bellet-Amalric, and B. Daudin, Appl. Phys. Lett. **92**, 201904 (2008).
²⁹Amit Pradhan, N. Y. Ma, and Feng Liu, Phys. Rev. B **70**, 193405 (2004).
³⁰B. Amstatt, O. Landré, V. Favre Nicolin, M. G. Proietti, E. Bellet-Amalric, C. Bougerol, H. Renevier, and B. Daudin, J. Appl. Phys. **104**, 063521 (2008).